Hybrid silica/polymer long period gratings for wavelength filtering and power distribution

Jiang, Jia; Callender, Claire L.; Noad, Julian P.; Ding, Jianfu

Publisher's version / Version de l'éditeur:
https://doi.org/10.1364/AO.48.004866
Applied Optics, 48, 26, pp. 4866-4873, 2009-09-10

Hybrid silica/polymer long period gratings for wavelength filtering and power distribution

Jia Jiang,[1,*] Claire L. Callender,[1] Julian P. Noad,[1] and Jianfu Ding[2]

[1]Communications Research Centre, P.O. Box 11490, Station H, Ottawa, Ontario K2H 8S2, Canada

[2]Institute for Chemical Process and Environmental Technology, National Research Council Canada, 1200 Montreal Road, Ottawa, Ontario K1A 0R6, Canada

*Corresponding author: jia.jiang@crc.gc.ca

Received 17 June 2009; revised 17 August 2009; accepted 17 August 2009; posted 18 August 2009 (Doc. ID 113003); published 1 September 2009

We report long period grating (LPG) devices based on a hybrid architecture incorporating photopatternable fluorinated poly(aryl ether ketone) and silica layers for applications in wavelength filtering and power distribution. The grating structure was implemented using a periodic corrugation on a thermally oxidized silica lower cladding layer, a photopatterned fluorinated polymer ridge waveguide, and a similar polymer top cladding. In this design, the corrugated silica layer allows a highly stable grating structure, while the fluorinated polymer offers a low propagation loss and easy processability. Strong rejection bands have been demonstrated in the C + L wavelength band, in good agreement with theoretical calculations. The fabricated LPG devices show a thermal dependence of 1.5 nm/°C. Based on this design, an array of waveguides incorporating LPGs has also been fabricated. Distribution of light at the resonance wavelength across all the channels from a single input has been demonstrated. These results are promising for power distribution in photonic network applications or on-chip sensors. © 2009 Optical Society of America

OCIS codes: 050.2770, 130.5460, 230.7390, 230.7408, 220.3740.

1. Introduction

Similar to Bragg gratings, long period gratings (LPGs) are formed by introducing a periodic variation of the effective refractive index along the waveguide structure; however, the pitch of an LPG is of the order of hundreds of micrometers, much longer than that of a Bragg grating. A LPG allows resonance light coupling between the guided mode and the cladding modes, resulting in a transmission spectrum consisting of a series of rejection bands at specific wavelengths. LPGs are attracting increasing interest in the areas of optical communication and photonic devices and have been demonstrated for applications such as band-rejection filters [1], gain flatteners for erbium-doped fiber amplifiers (EDFAs) [2], and dispersion compensators [3]. Also, due to the nature of the light coupling between the core and the cladding of the waveguides, LPGs are highly sensitive to environmental factors, showing promise in sensor applications in various fields, such as temperature, pressure, refractive index, and pH [4–8].

Fiber LPGs have been widely studied in the past few years. Several diverse fabrication techniques have been demonstrated. The most common and mature method is UV irradiation by a KrF excimer laser at 248 nm [1] or an Ar-ion laser at 244 nm [9] to create photochemically a refractive index periodic change along the fiber. This method requires a fiber that is highly photosensitive to the UV light in the radiation wavelength; typically Ge-doped silica fiber is employed. IR laser irradiation (using femtosecond pulses or a CO_2 laser) has also been used to successfully demonstrate gratings, by changing the refractive index of the fiber through compacting the material in the irradiated area [10,11]. Other fabrication methods include electric arc

0003-6935/09/264865-08$15.00/0

discharge [12], tapering [13], etching [14], or twisting [15], which induce the waveguide effective refractive index change by physically modifying the waveguide geometric structure. All these fabrication methods are limited by fiber physical and/or photochemical properties and may not offer much potential for mass production.

Similar to fiber gratings, the fabrication methods for planar grating waveguides can be based on chemically changing the material refractive index, e.g., through UV irradiation or ion implementation. However, unlike fiber, various photolithographically patterning methods can also be used, offering the advantage of the simultaneous fabrication of multiple devices on a wafer. Planar LPGs have been researched in detail and many literature contributions cover theoretical calculation and structure design [16,17] as well as grating implementation in various materials, ranging from glass to polymers [18–23]. LPGs have been demonstrated in benzocyclobutene ridge waveguides with the effective refractive index change induced by KrF excimer laser irradiation [18], in ion-exchanged BK7 glass slab waveguides [19], and other polymer waveguides by reactive ion etching [20] or by soft lithography [21]. Thermally induced refractive index modulation gratings have also been reported to exhibit strong wavelength rejection bands in polymer ridge waveguides [22,23]. In general, compared to fiber devices, planar LPG devices provide more flexibility in the selection of materials, refractive indices, and waveguide structures. They can also be integrated and packaged with other devices on silicon substrates, and can be produced in large quantities using standard microelectronic processing techniques.

In this paper, LPG planar waveguides have been designed and fabricated using a hybrid structure consisting of silica and polymer layers. A silica layer not only provides a low-loss and high-quality lower cladding, but also allows a corrugated periodic structure to be formed with precise dimensions via photolithography and reactive ion etching. The corrugated patterns ensure that the period structure has good stability in tough environments, such as exposure to higher temperature, humidity, and organic solvents. A new polymer material based on a highly fluorinated poly(arylether ketone) was selected to fabricate the waveguides and the upper cladding layer. The refractive index of this type of polymer can be adjusted during synthesis and it shows excellent thermal stability. It also has low optical absorption in the communication wavelength range than other optical polymers due to its high content of fluorine, and also has exhibited good photosensitivity to UV light. The latter property can be exploited to fabricate waveguide or grating structures by a simple and mature photolithography process. Several different photonic devices, including arrayed waveguide gratings [24] and Mach–Zehnder interferometers [25], have been demonstrated in our laboratory previously using this kind of polymer. The hybrid structure was chosen for the LPGs to take advantage of the unique properties of both silica and polymer layers. Theoretical calculations were carried out using commercially available modeling software (Optigrating and C2V TempSelene). By selecting the core/cladding material refractive index and waveguide geometry structure, resonance wavelengths within the C + L wavelength band could be calculated.

A single LPG exhibits a wavelength rejection band as the guided mode of the waveguide structure couples into the cladding modes. The light coupled into cladding modes can also be returned to the waveguide mode via a grating with the same period [26,27]. Since, theoretically, the cladding mode is distributed over the whole area of the cladding layer, the light could be coupled back into each individual guide if the same cladding layer covers the multiple guides incorporating identical LPGs, which are located in a relatively large area. Therefore, such a waveguide array could act as a signal distributor when light is input to only one single channel of the array. This phenomenon is different from the traditional directional coupler that depends on evanescent coupling between the waveguides, limited by the critical distance between the two waveguides. In this work, an array of LPG waveguides has been demonstrated with light distribution across every channel of the array.

2. Device Design and Simulation

A. Device Structure

Based on the polymer properties, the hybrid silica/polymer LPGs were designed and fabricated. A structure diagram of a cross section through a waveguide is presented in Fig. 1(a). This device is based on periodically corrugated shallow trenches on the

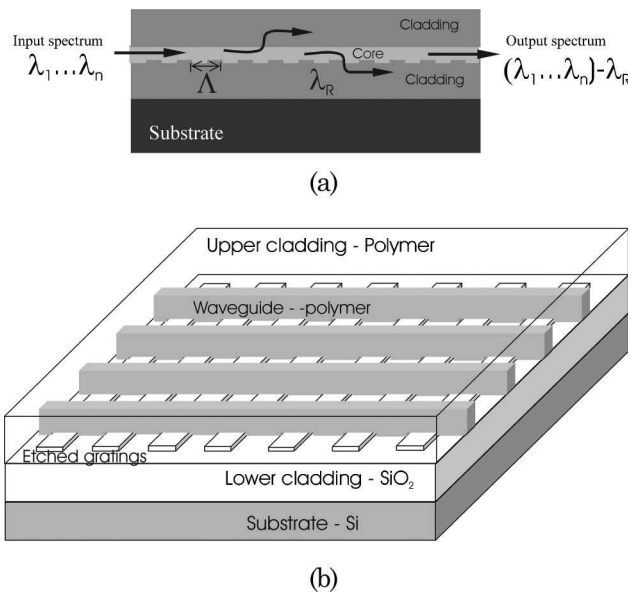

Fig. 1. (a) Grating structure based on the lower cladding corrugation, where Λ is the grating period and λ_R is the resonance wavelength. (b) Structure diagram of the LPG waveguide array.

lower cladding surface, which in turn transfer to the lower surface of the polymer ridge waveguides. The periodic dimensional variation of the waveguide structure leads a correspondingly periodic change in the waveguide effective index, resulting in a grating resonance at a specific wavelength at which light couples into the cladding layers. The waveguide core was fluorinated poly(aryl ether ketone), in the form of a ridge fabricated by a photopatterning and wet-etching process. In order to get a good match of material properties, the top layer was a fluorinated poly (aryl ether ketone) polymer of a lower index.

The structure of the LPG waveguide array is depicted in Fig. 1(b). Multiple ridge waveguides are located on the entirely corrugated lower cladding layer. The distance between the ridges is up to 100 μm and the number of the waveguides is typically ten. The input light is introduced via a single-mode fiber into one of the waveguides, typically the middle one in the array. The transmitted light can then be observed in the neighboring channels.

B. Simulation

The resonance wavelength, denoted as λ_R, is given by the grating matching condition:

$$\lambda_R = (N_{\mathrm{co}} - N_{\mathrm{cl}})/\Lambda, \tag{1}$$

where N_{co} and N_{cl} are the effective index of the guided mode and the cladding modes of the structure, respectively, and Λ is the grating period. Figure 2 shows the relationship between the resonance wavelength and the grating period of the LPG, calculated using the finite difference method within the OlympIOs C2V software. The calculation is based on a 6 μm wide and 3 μm high waveguide ridge (6 μm × 3 μm) with 6 μm thick upper cladding. The core material refractive index is 1.5330(TE)/1.5302(TM) (measured with a prism coupler at 1550 nm), and the upper cladding refractive index is 0.025 lower than that of the core. The aim is to fabricate a LPG with a resonance wavelength centered in the range of 1500–1600 nm. A grating period in the range of 70–180 μm gives a resonance in this wavelength range for different cladding modes. In this paper, all the simulation and experimental results are presented for TM polarization only. Results for TE polarization are generally similar, but shifted in wavelength due to the birefringence of the waveguide structure.

Cladding thickness is an important factor affecting the LPG resonance wavelength. As all the waveguides in this paper were fabricated on a 15 μm thick SiO_2 layer that forms the lower cladding layer, which was grown on a silicon wafer, we only considered the upper cladding influence on the grating properties. Figure 3(a) exhibits the function curves of period and resonance wavelength with various cladding thickness over a range of about 1 μm. Figure 3(b), which shows the same data set for an LPG with period 180 μm, demonstrates that the resonance

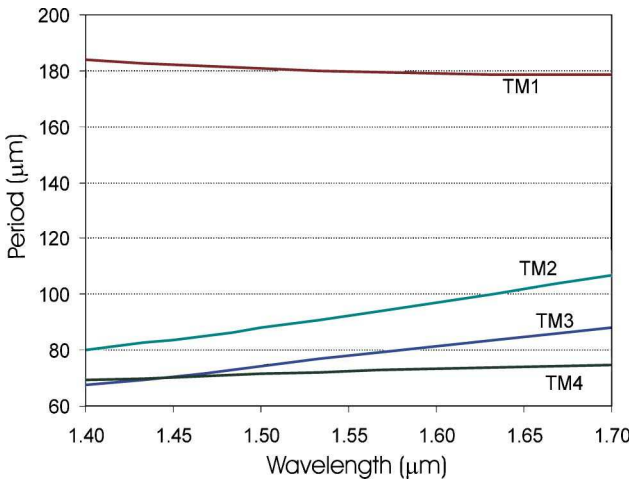

Fig. 2. (Color online) Resonance wavelength as a function of grating period for the fundamental core mode to the first four cladding modes of a 6 μm × 3 μm waveguide with a 6 μm thick upper cladding.

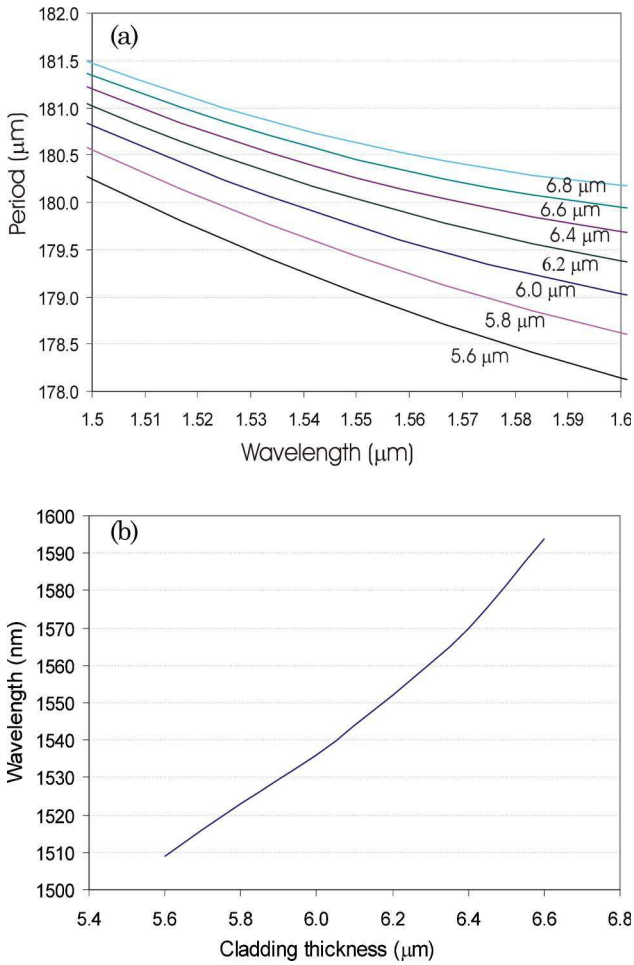

Fig. 3. (Color online) (a) Simulation of the period as a function of resonance wavelength for the 6 μm × 3 μm waveguide for $TM_0 \rightarrow TM_1$ with cladding thickness ranging from 5.8 to 6.8 μm. (b) Simulation of the resonance wavelength as function of cladding thickness for the 6 μm × 3 μm waveguide for $TM_0 \rightarrow TM_1$ at a period of 180 μm.

wavelength is highly sensitive to the cladding thickness. shifting to the red as the thickness increases. It is clear from these results that, to consider LPGs for sensor applications, cladding thickness is one of the most important factors that must be appropriately controlled.

3. Device Fabrication

A. Materials

Traditional optical poly(aryl ether ketone) polymers do not typically exhibit sufficient UV sensitivity to facilitate photolithographic patterning. Ridge waveguides realized using this kind of polymer are usually fabricated by dry-etching processes, such as reactive ion etching. However, for the newly designed fluorinated poly(arylether ketone) used in this work, a high content of vinyl groups has been introduced into the polymer molecule. With the presence of a suitable photoinitiator and photosensitizer, polymer cross-linking could be easily induced in the unsaturated tetrafluorostyrol groups after UV exposure at 365 nm. A wet chemical process developed the ridge waveguides in the cross-linking area. This newly synthesized fluorinated poly(aryl ether ketone) has an average molecular weight in the range of 25,000–35,000; a polydispersity of 2.6–4.6; excellent solubility in common organic solvents, such as cyclohexanone, tetrahydrofuran (THF), or acetone; and has a high glass transition temperature in the range of 150–185 °C. Thermal gravimetric analysis (TGA) measurements exhibited very high thermal stability as assessed by the temperature of 5% weight loss (e.g., up to 480 °C in nitrogen). The refractive index can be tailored from 1.50 to 1.53 by changing the feed ratio of monomers.

B. Fabrication

For the LPG based on the structure in Fig. 1, the lower cladding is formed by thermally oxidizing the silicon wafer using a standard oxidation process. The silica layer is controlled to 15 μm thick and has a refractive index of 1.4450(TE)/1.4455(TM) at a wavelength of 1.55 μm . Periodic patterns in photoresist were produced on the silica layer through a photolithography process that opens windows in the photoresist. Reactive ion etching then was used to transfer the patterns to the silica layer. The resultant grating structure has a ridge height of 100 nm and a period duty cycle of 50%. Figure 4 shows the scanning electron microscope (SEM) picture of the corrugated silica layer.

The core layer was formed from a fluorinated poly(aryl ether ketone) solution in cyclohexanone solvent containing the free radical photoinitiator 2-(4-methoxystyryl)-4,6-bis(trichloromethyl)-1,3,5-triazine (MSTA) and a photosensitizer, 2-chlorothioxanthen-9-one (CTX) to facilitate the photo cross-linking process through the tetrafluorostyrene moieties present in the polymer side chain. Photosensitive films with a typical thickness of 3–6 μm

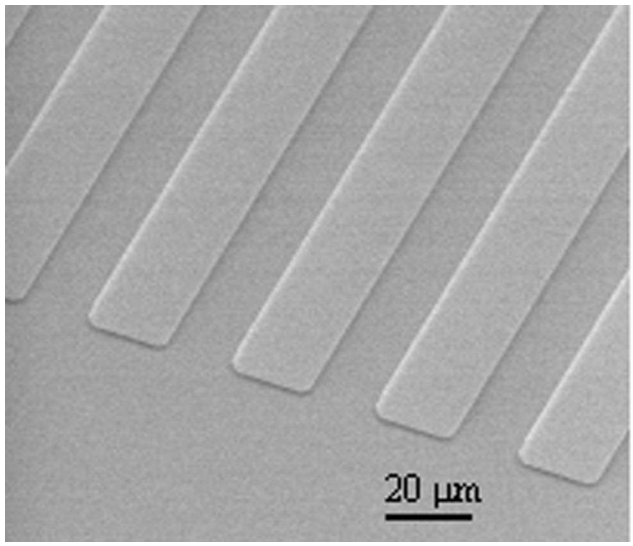

Fig. 4. SEM picture of etched lower SiO_2 cladding layer; the height of the patterns is 100 nm.

were deposited on thermally oxidized silicon substrates by spin coating. The films were prebaked in air at 130 °C for 10 min on a hotplate, then exposed to UV light at 365 nm through a mask, in a similar manner to a conventional photolithography process. Following postexposure baking at 150 °C for 10 min in an oven, the sample was developed in tetrahydrofuran and acetone, and rinsed with isopropyl alcohol to leave the desired ridges, which form the core of the waveguide structure. The waveguide ridge and sidewall profiles were evaluated using a SEM. The resultant ridge is shown in Fig. 5. An upper cladding layer was finally deposited on the sample by spin coating a similar polymer to complete the waveguide structure.

C. Characterization

The fabricated LPGs were characterized by launching light from a tunable laser at 1500–1600 nm into the waveguide from a standard single-mode fiber, and monitoring the output on a infrared camera

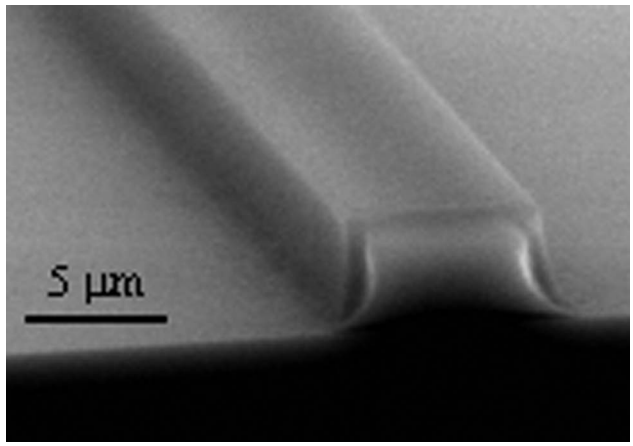

Fig. 5. SEM picture of photopatterned ridge waveguide with the photosensitive poly(aryl ether ketone) prior to coating cladding.

and a photodetector. The optical loss of the straight waveguides was estimated with the cutback method, that is, measuring the transmitted optical power in successively shorter lengths of a straight ridge waveguide. The uncertainty associated with this technique is about $\pm 0.2\,\mathrm{dB/cm}$ in our measurements, which can be attributed to the scattering in the points for the regression fit used to estimate the propagation loss due to the coupling variation between the fiber and waveguide endface. Low losses of about 0.5–0.6 dB/cm for the waveguide were obtained. Compared to the slab loss of 0.4–0.5 dB/cm [25] that we have measured using the high-index liquid immersion technique, this fabrication process does not introduce any significant additional loss.

4. Results and Discussion

A. Single LPG Transmission

To obtain a rejection peak located within the C + L wavelength band, a period of 180 μm was chosen for the corrugated lower cladding layer. This value is based on the relationship between the resonance wavelength and the grating period that was calculated according to Eq. (1) using the structure effective index. Figure 6(a) presents the transmission spectra of the device from both simulations and experimental measurements. The simulation was based on the waveguide parameters of the fabricated devices. The data indicate clearly that the experimental results and the simulation curve are in good agreement at the resonance wavelength. Similarly, the resonance wavelength and the grating period have been calculated based on the waveguide experimental data, as shown in Fig. 6(b). The calculation identified that the resonance wavelength at 1530 nm should correspond to the coupling and copropagation of the TM_0 and TM_1 modes. The resonance depth is related to the overlap ratio of the modes, as well as to the LPG length. Deviation of the experimental resonance depth from the simulated result may be attributed to preparation of the devices by manual cleaving of the silicon wafer through the LPG structure, which can cause variations in the waveguide endface or/and the LPG length.

As mentioned above, the coupling of light at the resonance wavelength into the cladding in LPG waveguides creates a high sensitivity of the LPG device to the surrounding temperature. Since polymer materials have a much larger thermo-optic coefficient than inorganic materials, a small temperature variation can induce a large shift in the LPG resonance wavelength of these hybrid devices. Figures 7 and 8 present experimental measurements of the resonance wavelength shift with increasing temperature. The resonance dip moves to longer wavelengths with increasing temperature; the slope of the wavelength-versus-temperature function is 1.5 nm/°C. This value is higher than that of a long period silica fiber grating (0.3 nm/°C) [4], but smaller than the sensitivities measured for other hybrid devices, such as epoxy-polymer-clad ion-exchanged BK7 glass waveguides (9.0 nm/°C) [19]. This temperature sensitivity relaxes the fabrication tolerances by allowing final adjustment and control of the device response to be made thermally. It is also sufficient to offer thermal tuning of the rejection band over a wide wavelength range (60 nm or more in the C + L band for a temperature change of 40 °C), a key capability for practical wavelength filters.

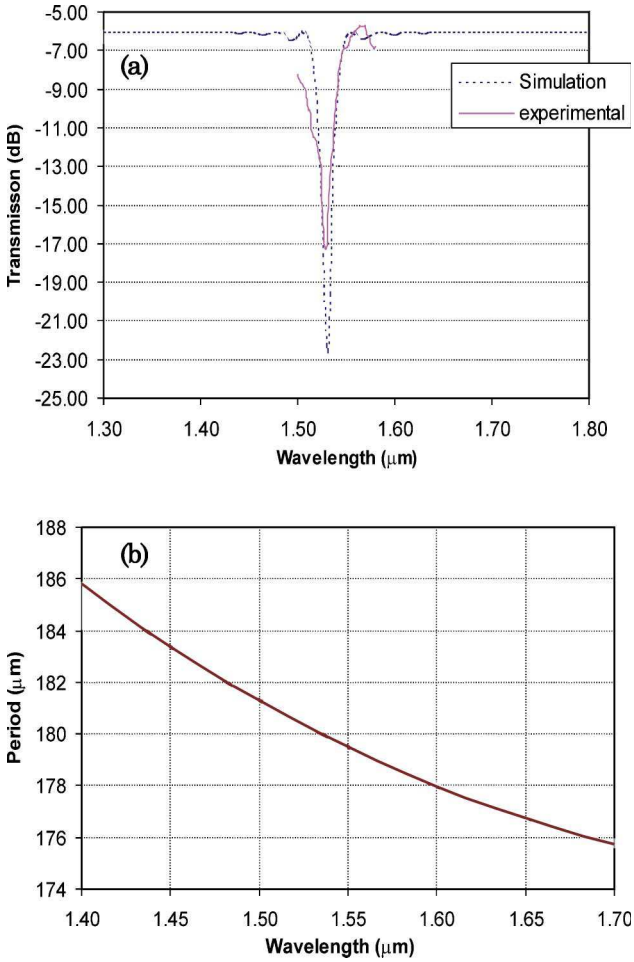

Fig. 6. (Color online) (a) Transmission spectrum (TM polarization) for a typical LPG (waveguide size 6.2 μm × 3.2 μm with average cladding thickness 6.4 μm and length 28 mm). Experimental data, solid curve; simulation data, dotted curve. (b) Calculated relationship between period and wavelength for the LPG in (a).

This hybrid silica/polymer LPG offers the dual advantages of the temperature sensitivity of polymer materials coupled with the superior stability of a physically corrugated grating structure as compared to UV-induced gratings in all-polymer devices. Some UV-irradiation-induced planar LPGs based on this fluorinated poly(arylether ketone) and photosensitive polymer upper cladding have been investigated in our laboratory recently. It was found that their spectral responses varied uncontrollably with environmental factors. In the UV-induced gratings, increasing temperature or extended periods at relatively high temperatures would cause the index

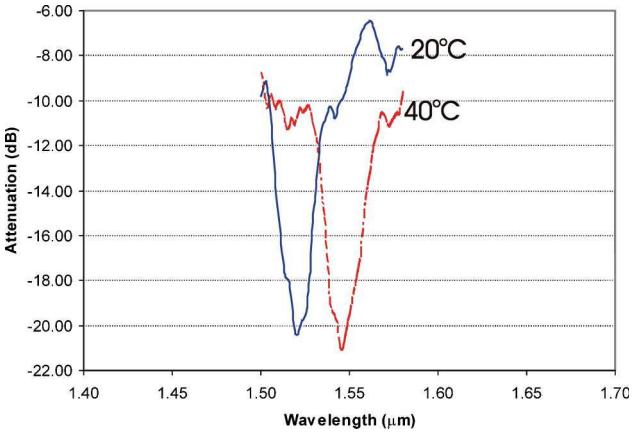

Fig. 7. (Color online) Wavelength shift of the fabricated hybrid polymer/silica LPG at 20 °C and 40 °C.

modulation to change or even disappear, leading to significant changes in the transmission spectra. This work reinforced the conclusion that the hybrid structure with a grating formed by physical corrugation is more suitable for practical applications, such as wavelength filtering.

B. Multiple Channel Coupling

An optical coupler based on two parallel LPG fibers has been demonstrated theoretically and experimentally for band-rejection and bandpass filters [28]. However, this kind of device presents challenges in packaging and in the fabrication of multichannel arrays. Planar LPG arrays fabricated on the same substrate offer advantages for this type of device. Theoretical calculation and experimental fabrication demonstrated that light could be transferred effectively between widely separated parallel LPG waveguides over a short distance [26,27]. This light transfer is different from traditional directional couplers in which light is evanescently coupled between two closely spaced waveguides. In a planar LPG array, the light is coupled into the whole cladding layer through the gratings in the input waveguide, then coupled back to the other waveguides in the array that have a grating of the same period. This type of array LPG device functions over much larger coupling distances than the traditional directional coupler. Furthermore, the large distance between channels allows more flexibility and tolerance in the device fabrication, while offering a highly effective method of distributing optical signals. In this work, a planar LPG array structure was achieved using the same hybrid structure based on low-loss fluorinated poly(arylether ketone) on a silica corrugated cladding layer. The waveguide array has been fabricated with waveguide ridges separated by a distance of 100 μm. For this distance, this coupling cannot be from the evanescent coupling between waveguides as in a traditional optical coupler.

As shown in Fig. 1(b), the waveguide array was fabricated on the etched lower silica cladding. For a ten-waveguide array, the grating area is distributed over a distance of about 1000 μm. Light was input via butt coupling from a single-mode fiber into one waveguide in the array, typically one near the center. The transmitted light could be observed in all the other channels in the array. Figure 9 shows an infrared camera image of the output of the array and Fig. 10 the power intensity distribution, both at resonance wavelength. Light can be seen in all fabricated channels. This result demonstrates the uniformity of the fabricated waveguides, because any slight variation of the ridge geometry and cladding thickness can prevent the light in the cladding layer from coupling back to the other waveguides [27]. However, the experiment observed that the transmitted power in the input channel became weaker, but did not disappear as desired. This probably indicates that the input power at the resonance wavelength did not couple completely into the cladding or, alternatively, part of the optical power in the cladding mode has also coupled back to this input waveguide. A slight deviation from the design values of waveguide structure parameters, such as refractive index and physical dimensions, could result in incomplete coupling of light at the resonance wavelength into the cladding. Furthermore, the LPG length may be an important factor in the coupling

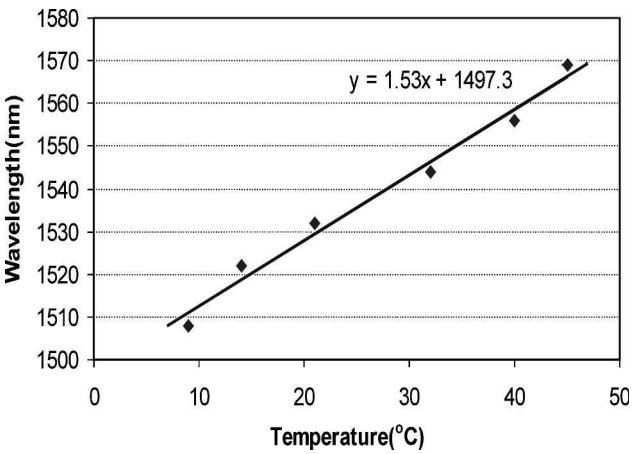

Fig. 8. Temperature dependence of the fabricated polymer/silica hybrid LPG.

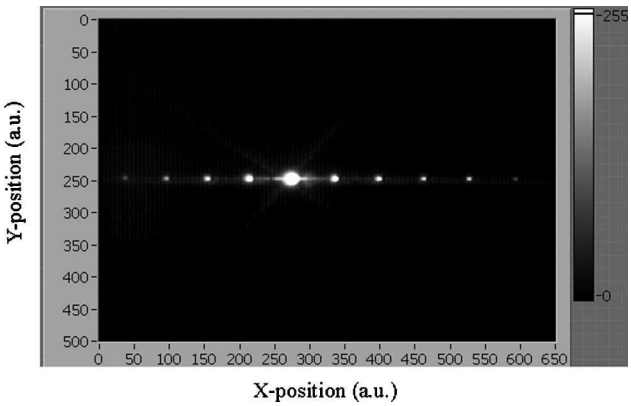

Fig. 9. Output light distribution in a ten-waveguide LPG array, as captured on an infrared camera.

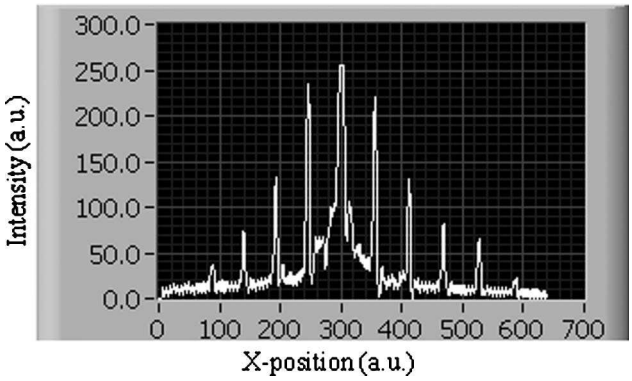

Fig. 10. Light intensity from the ten-waveguide grating array.

efficiency since the light may couple in and out of the waveguide several times along a given length. In the characterizations, the multichannel outputs have only been observed in certain lengths of samples. In this case, shown in Figs. 9 and 10, it was about 30 mm.

The wavelength dependence has been characterized and typical results are exhibited in Fig. 11. The upper curve in Fig. 11 shows the transmission spectra of the input channel, which was the fifth waveguide in the array. There is a resonance peak located at 1524 nm with an attenuation of ~ – 20 dB. The wavelength was then scanned for each of the other channels in the array. Four typical spectra, noted as R1, L1, L2, and the input channel are presented in Fig. 11. Curve R1 is from the channel immediately to the right of the input waveguide, and curves L1 and L2 are from those immediately to the left. The spectra indicate clearly that the transmission intensity increased at the rejection wavelength of the input channel. Based on these results, the LPG array exhibits good potential for the application of power distribution. Work is ongoing to further refine these devices and fully control the parameters that determine the rejection bands and light distribution.

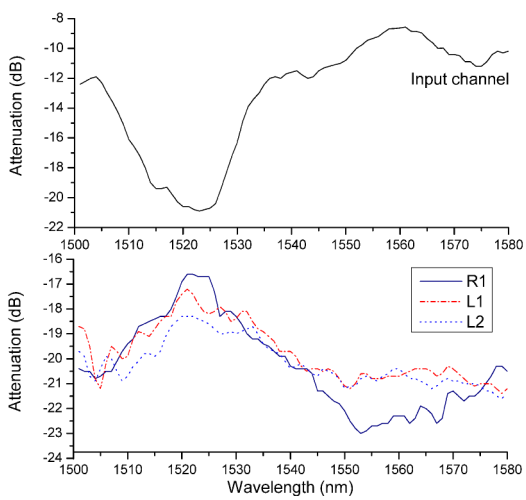

Fig. 11. (Color online) Spectra of the planar grating array. Upper curve is from the input channel; Curve R1 is from the channel immediately to the right of the input waveguide; curves L1 and L2 are from those immediately to the left.

5. Summary

Planar LPGs based on hybrid polymer and silica materials have been demonstrated. The grating is formed by physical corrugation in the silica lower cladding layer, providing advantages of good grating stability, easy processability, and design flexibility. Well-defined rejection bands have been detected at resonance wavelengths that are in good agreement with theoretical calculations. LPG waveguide arrays have been successfully demonstrated, with light distributed across multiple channels from a single input. The output intensity is strongly correlated with the resonance wavelength. These results demonstrate the potential application of hybrid silica/polymer LPGs and LPG arrays for low-cost and easily fabricated planar integrated wavelength filters, sensors, and on-chip power distribution.

References

1. A. M. Vengsarkar, P. J. Lemaire, J. B. Judkins, V. Bhatia, T. Erdogan, and J. E. Sipe, "Long-period fiber gratings as band-rejection filters," J. Lightwave Technol. **14**, 58–65 (1996).
2. A. P. Zhang, X.-W. Chen, J.-H. Yan, Z.-G. Guan, S. He, and H.-Y. Tam, "Optimization and fabrication of stitched long-period gratings for gain flattening of ultrawide-band EDFAs," IEEE Photon. Technol. Lett. **17**, 2559–2561 (2005).
3. M. Das and K. Thyagarajan, "Dispersion compensation in transmission using uniform long period fiber gratings," Opt. Commun. **190**, 159–163 (2001).
4. A. P. Zhang, L.-Y. Shao, J.-F. Ding, and S. He, "Sandwiched long-period gratings for simultaneous measurement of refractive index and temperature," IEEE Photon. Technol. Lett. **17**, 2397–2399 (2005).
5. D. E. Ceballos-Herrera, I. Torres-Gómez, A. Martínez-Ríos, G. Anzueto-Sánchez, J. A. Álvarez-Chávez, R. Selvas-Aguilar, and J. J. Sánchez-Mondragón, "Ultra-widely tunable long-period holey-fiber grating by the use of mechanical pressure," Appl. Opt. **46**, 307–311 (2007).
6. L. Su, K. S. Jiang, and C. Lu, "CO_2-laser-induced long-period gratings in graded-index multimode fibers for sensor applications," IEEE Photon. Technol. Lett. **18**, 190–192 (2006).
7. S. T. Lee, R. D. Kumar, P. S. Kumar, P. Radhakrishnan, C. P. G. Vallabhan, and V. P. N. Nampoori, "Long period gratings in multi-mode optical fibers: application in chemical sensing," Opt. Commun. **224**, 237–241 (2003).
8. K. Wang, D. Klimov, and Z. Kolber, "Seawater pH sensor based on the long period grating in a single-mode-multimode-single-mode structure," Opt. Eng. **48**, 034401 (2009).
9. V. Bhatia, D. Campbell, R. O. Claus, and A. M. Vengsarkar, "Simultaneous strain and temperature measurement with long-period gratings," Opt. Lett. **22**, 648–650 (1997).
10. P. Lu, D. Grobnic, and S. J. Mihailov, "Characterization of the birefringence in fiber Bragg gratings fabricated with an ultrafast-infrared laser," J. Lightwave Technol. **25**, 779–786 (2007).
11. V. Grubsky and J. Feinberg, "Fabrication of axially symmetric long-period gratings with a carbon dioxide laser," IEEE Photon. Technol. Lett. **18**, 2296–2298 (2006).
12. G. M. Rego, J. L. Santos, and H. M. Salgado, "Refractive index measurement with long-period gratings arc-induced in pure-silica-core fibres," Opt. Commun. **259**, 598–602 (2006).

13. L.-Y. Shao, J. Zhao, X. Dong, H. Y. Tam, C. Lu, and S. He, "Long-period grating fabricated by periodically tapering standard single-mode fiber," Appl. Opt. **47**, 1549–1552 (2008).
14. N. Chen, B. Yun, and Y. Cui, "Cladding index modulated fiber grating," Opt. Commun. **259**, 587–591 (2006).
15. V. I. Kopp, V. M. Churikov, J. Singer, N. Chao, D. Neugroschl, and A. Z. Genack, "Chiral fiber gratings," Science **305**, 74–75 (2004).
16. V. Rastogi and K. S. Chiang, "Long-period gratings in planar optical waveguides," Appl. Opt. **41**, 6351–6355 (2002).
17. Q. Liu, K. S. Chiang, and V. Rastogi, "Analysis of corrugated long-period gratings in slab waveguides and their polarization dependence," J. Lightwave Technol. **21**, 3399–3405 (2003).
18. Q. Liu, K. S. Chiang, and K. P. Lor, "Long-period gratings in polymer ridge waveguides," Opt. Express **13**, 1150–1160 (2005).
19. K. S. Chiang, K. P. Lor, C. K. Chow, H. P. Chen, V. Rastogi, and Y. M. Chu, "Widely tunable long-period gratings fabricated in polymer-clad ion-exchanged glass waveguides," IEEE Photon. Technol. Lett. **15**, 1094–1096 (2003).
20. M.-S. Kwon and S.-Y. Shin, "Refractive index sensitivity measurement of a long-period waveguide grating," IEEE Photon. Technol. Lett. **17**, 1923–1925 (2005).
21. A. Perentos, G. Kostovski, and A. Mitchell, "Polymer long-period raised rib waveguide gratings using nano-imprint lithography," IEEE Photon. Technol. Lett. **17**, 2595–2597 (2005).
22. M.-S. Kwon and S.-Y. Shin, "Tunable notch filter using a thermo-optic long-period grating," J. Lightwave Technol. **22**, 1968–1975 (2004).
23. M.-S. Kwon and S.-Y. Shin, "Polymer waveguide notch filter using two stacked thermooptic long period gratings," IEEE Photon. Technol. Lett. **17**, 792–794 (2005).
24. Y. Qi, J. Jiang, C. L. Callender, M. Day, and J. Ding, "Cross-linkable bromo-fluorinated poly(arylene ether ketone)s for photonic device applications," Appl. Opt. **45**, 7480–7487 (2006).
25. J. Jiang, C. L. Callender, J. P. Noad, Y. Qi, J. Ding, and M. Day, "Photopatterning of waveguide devices using fluorinated poly(arylene ether ketone)," Opt. Eng. **46**, 074601 (2007).
26. Y. Bai and K. S. Chiang, "Analysis of long-period waveguide grating arrays," J. Lightwave Technol. **24**, 3856–3863 (2006).
27. Y. Bai, Q. Liu, K. P. Lor, and K. S. Chiang, "Widely tunable long-period waveguide grating couplers," Opt. Express **14**, 12644–12654 (2006).
28. K. S. Chiang, F. Y. M. Chan, and M. N. Ng, "Analysis of two parallel long-period fiber gratings," J. Lightwave Technol. **22** (5), 1358–1366 (2004).